Aging and Transformation of Polyethylene Microplastics in UASB Effluents Treated with O₃ and O₃/H₂O₂: Physicochemical Changes and Toxicity Assessment

Diego A. S. Brito, Thalita F. Silva, Priscila S. Cavalheri, Antonio K. Canatto, Emmanuel S. C. Miguel, Fernando Jorge C. M. Filho, Lincoln C. S. Oliveira, Gleison A. Casagrande, and Amilcar M. Junior*



Cite This: ACS EST Water 2025, 5, 6830-6841

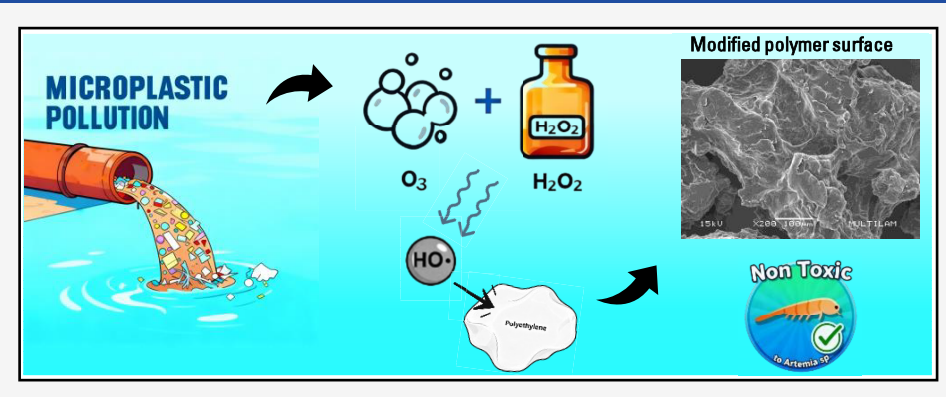


ACCESS I

III Metrics & More

Article Recommendations

Supporting Information



ABSTRACT: Wastewater treatment plants (WWTPs) represent a pathway for microplastics (MPs) to enter the environment, through direct discharge via effluents into surface waters or indirect release via sewage sludge applied to agricultural soils. This study demonstrates the effectiveness and safety of an O₃/H₂O₂ process for aging polyethylene microplastics (PE-MPs) directly within a complex UASB reactor effluent. A characteristic FTIR peak at 1714 cm⁻¹ confirms the formation of carbonyl groups, which indicates that the treatment caused significant surface degradation under optimal conditions (52.00 mg L⁻¹ O₃ and 100.00 mg L⁻¹ H₂O₂ for 110 min). Crucially, the byproducts produced showed no acute toxicity to Artemia salina, demonstrating that the process was environmentally sound. Additionally, thermogravimetric analysis (TGA) revealed a counterintuitive increase in the polymer's thermal stability, suggesting complex structural reorganization potentially driven by the removal of low-molecular weight fractions or cross-linking. Treated PE exhibited increased thermal stability, increasing from 436.18 to 449.35 °C, indicating that the remaining fragments are more thermally resistant and could therefore alter their subsequent fragmentation behavior. This work, therefore, validates a robust and safe strategy for MP remediation in realistic scenarios.

KEYWORDS: ozonation, emerging pollutants, design of experiments, advanced oxidation processes, toxicity

1. INTRODUCTION

The remarkable versatility of plastics has led not only to their widespread use but also to alarming accumulation in aquatic environments, with projections indicating that 250 million tons of plastic waste will contaminate water bodies worldwide by 2025. This waste fragments into microplastics (MPs), particles smaller than 5 mm, which pose significant risks to their environmental persistence and potential for bioaccumulation.²⁻⁴ Studies confirm that PE-MPs can induce significant tissue damage in aquatic organisms, such as gill inflammation in fish, and may also enhance ecotoxicity by acting as vectors for emerging pollutants and heavy metals.2

Wastewater treatment plants (WWTPs) represent a primary pathway for MPs entering aquatic environments, 5,6 since these facilities are not explicitly designed to remove such pollutants WWTPs receive a constant influx of MPs from domestic and industrial sources, including textile fibers, microbeads from personal care products, and particles from tire wear, 8-11 a single facility can release approximately 65 million microplastic particles daily. 12-15 Furthermore, retained MPs accumulate in treatment sludge, creating a risk of transfer to terrestrial environments via agricultural application, 16 while landfill leachates provide another contamination source to

Received: July 2, 2025 Revised: October 21, 2025 Accepted: October 22, 2025

Published: October 29, 2025







Figure 1. Location and sampling point of the effluent used in this study. Satellite image of the Los Angeles Municipal WWTP (red outline).

WWTPs.¹⁷ The development of effective remediation technologies for MPs in WWTPs is still an emerging field.¹⁸

Current strategies for MPs removal present challenges: in drinking water treatment plants, filtration units such as rapid sand filters or microfiltration membranes, although primarily designed to remove suspended solids and residual particulates, have been reported to subject MPs to mechanical stress caused by shear forces, turbulence, and hydraulic surges. Under such conditions, larger microplastics can fragment into smaller particles, often \leq 20 μ m, thereby increasing the proportion of fine MPs in the treated water. 19 Biological degradation, although demonstrated for specific bacteria and fungi, ^{20,21} is generally too slow for practical, large-scale applications. To address these gaps, advanced oxidation processes (AOPs) have emerged as a promising alternative. AOPs, which generate highly reactive hydroxyl radicals (HO*), are effective for degrading a wide range of recalcitrant pollutants, including pesticides, ^{22,23} pharmaceuticals, ^{24–27} endocrine-disrupting compounds, ²⁸ MPs, ²⁹ and others. ^{30,31} These processes offer key advantages, such as rapid reaction rates and the potential for complete mineralization, making them versatile and practical remediation technologies. 32,33

Among AOPs, ozone-based methods have been reported as particularly effective. Ozone (O_3) , especially when combined with hydrogen peroxide (H_2O_2) , has been shown to enhance the generation of HO^{\bullet} radicals.²⁸ These radicals initiated oxidative reactions by attacking the polymer backbone, thereby promoting chain scission and fragmentation, as well as the

formation of oxygen-containing functional groups like carbonyls and hydroxyls. The presence of these groups, in turn, increased the hydrophilicity and reactivity of the polymer surface. However, a critical gap has remained in the literature, since most AOP studies on MPs utilize simplified matrices such as deionized water, failing to account for the complex interactions present in real effluents. This issue resulted from matrix complexity, including the presence of dissolved organic matter, humic substances, inorganic ions, and potential radical scavengers, which could both inhibit the generation of HO• and reduce the aging effects on MPs, as these radicals might react with other species present.

Polyethylene microplastics (PE-MPs) were selected as the target material in this study due to their widespread occurrence in wastewater and both marine 42 and freshwater environments. 6,18 To address this, the aging of PE-MPs was investigated in the present study through an $\rm O_3/H_2O_2$ treatment applied to real effluent from an Upflow Anaerobic Sludge Blanket (UASB) reactor. A factorial experimental design was employed to optimize the process conditions, while MPs were characterized by using analytical techniques, including Scanning Electron Microscopy (SEM), Fourier-Transform Infrared Spectroscopy (FTIR), and Thermogravimetric Analysis (TGA). Additionally, Artemia salina ecotoxicity assays were conducted to comprehensively evaluate both the treatment efficiency and its environmental safety.

2. MATERIALS AND METHODS

2.1. Reagents. Polyethylene microplastics (PE-MPs; \approx 600 μ m, pellets, natural white, additive-free) were purchased from Bianquimica (São Paulo, Brazil). Hydrogen peroxide (30% v/v, Vetec), sulfuric acid (98%, Dinâmica), sodium hydroxide (99%, Merck), potassium iodide (99%, Vetec), and potassium dichromate (99% Dinâmica). Ultrapure water (conductivity <0.05 μ S cm⁻¹ at 25.00 °C) from a Gehaka DG500 UF system was used in all experiments.

2.2. Effluent Characterization. The effluent used in the experiments was collected from the outlet of a UASB reactor at the Los Angeles Municipal Wastewater Treatment Plant (WWTP) in Campo Grande, MS, Brazil ($20^{\circ}33'27''S$, $54^{\circ}39'24''W$; Figure 1). The plant treats 1100 L s^{-1} , responsible for treating about 90% of the effluent generated by the municipality, including drainage and sewage, as well as leachate produced by the municipal landfill with an average flow rate of 5.05 L s^{-1} , corresponding, throughout the day, to 1.0% of the total effluent of municipal sewage and discharges to the Anhandui River (Class IV).

Table 1 shows the physicochemical parameters evaluated for the characterization of the effluent. All parameters were

Table 1. Physicochemical Characteristics of the Post-UASB Effluent

physicochemical parameter ^a	method	unit	value	release limit standard ^b
temperature	_	°C	27.20 ± 4.40	<40.00
pН	4500 B	_	7.00 ± 0.50	6.00-9.00
turbidity	2130 B	NTU	28.50 ± 12.00	_
total nitrogen	4500 C	$mg\ L^{-1}$	21.10 ± 3.20	_
nitrite	4500 B	$mg\ L^{-1}$	2.40 ± 1.30	-
nitrate	4110 B	$mg L^{-1}$	2.80 ± 0.80	_
ammonia nitrogen	4500 B and C	$mg L^{-1}$	4.40 ± 1.20	20.00
total phosphorus	4500 B5 and 4500 E	mg L ⁻¹	4.40 ± 0.90	_
total solids	2540 B	$mg\ L^{-1}$	674.00 ± 122.70	_
COD	5220 B	$mg\ L^{-1}$	338.50 ± 8.00	_
BOD	5210 B	$mg\ L^{-1}$	68.90 ± 40.00	<120.00
TOC	_	$mg L^{-1}$	26.00 ± 1.30	_

 $^{\alpha}n=14$ samples corresponding to independent monthly collections over a 14-month period. Each sample was collected at the WWTP outlet and preserved by refrigeration (\sim 4 °C). Values represent raw means of the 14 independent measurements, with the standard deviation reflecting temporal variability across months. No statistical test for sample homogeneity was applied, and no outliers were excluded. TOC = total organic carbon. COD = chemical oxygen demand. BOD = biochemical oxygen demand. b Discharge limit values for class IV rivers. 44 No limits are established for turbidity, total nitrogen, nitrite, nitrate, total phosphorus, total solids, COD, or TOC.

determined according to the Standard Methods for the Examination of Water and Wastewater. 43

The post-UASB reactor effluent was chosen as the most suitable point for the application of AOPs before discharge, allowing the assessment of whether induced aging promotes physicochemical changes in PE-MPs that enhance their biodegradability and reduce their environmental persistence.

2.3. Aging Experiments. The aging of PE-MPs was carried out using ozone (O_3) and a combined ozone/hydrogen peroxide (O_3/H_2O_2) system. Each experimental run consisted

of a 300 mg suspension of PE-MPs in 300 mL of either ultrapure water or post-UASB reactor effluent. The effluent was used directly as collected, without filtration or any other pretreatment.

The experiments were conducted in a 500 mL glass beaker. Mixing was achieved by bubbling ozone vigorously through a fine-pore diffuser (Figure S1 and S2, see Supporting Information), ensuring homogeneous contact between the particles, oxidants, and the aqueous matrix. Ozone was generated *in situ* from industrial-grade oxygen using an ozonizer (0&L 10.0 RMSO2, OZONE & LIFE). The ozone concentration range in the aqueous phase (34–52 mg L⁻¹) was based on oxygen feed rates of 0.5–1.5 L min⁻¹.

For the aging experiments conducted with the O_3/H_2O_2 process, H_2O_2 was added at the beginning of the reaction. The investigated H_2O_2 concentration ranged from 30.00 mg L⁻¹ to 100.00 mg L⁻¹, based on preliminary and previous studies. ^{26,45} The experiments were conducted without pH adjustment in either ultrapure water or effluent (pH 7.00 \pm 0.50 for the post-UASB reactor effluent; Table 1), as initial tests indicated negligible variation between acidic and neutral conditions ($\Delta TOC = 0.02$ mg L⁻¹).

At the end of each aging experiment, PE-MPs were recovered for FTIR, SEM, and TGA analysis. Recovery was performed by filtration using qualitative filter paper (pore size 4-12 μ m, 80 g/m²). The recovered solids were dried in a desiccator at room temperature for approximately 48 h. To monitor the aging process, PE-MPs were sampled at predetermined time intervals (0, 10, 60, and 110 min). The release of soluble organic compounds from PE-MPs during aging was tracked by total organic carbon (TOC). For this analysis, collected aliquots were filtered through a 0.22 μm PTFE filter, and the filtrate was analyzed using a Shimadzu TOC VCPN analyzer. The change in TOC (Δ TOC) was calculated as TOC_{final} - $TOC_{initial}$, where $TOC_{initial}$ corresponds to the TOC measured at t = 0 (immediately after PE-MPs addition and before oxidant introduction), and TOC_{final} is the TOC measured at the end of the reaction time. This Δ TOC value represents the increase in filtered, nonvolatile organic carbon. 46 A calibration curve was prepared using potassium hydrogen phthalate (C₈H₅O₄K) over a range of 2.00-100.00 mg L^{-1} , yielding the equation TOC = (Area -1.2919)/0.42067 with a coefficient of determination (R2) of 0.9998. The method provided limits of quantification (LOQ) and detection (LOD) of 0.18 mg L^{-1} and 0.05 mg L^{-1} , respectively, with a measurement precision of \pm 2%.

The optimized variables were then applied to the post-UASB reactor effluent to carry out the characterization of PE-MP aging by FTIR, SEM, and TGA.

The residual dissolved ozone concentration (mg L^{-1} was quantified using the iodometric titration method. Aliquots of the reaction mixture were bubbled into a 0.10 mol L^{-1} potassium iodide (KI) solution under acidic conditions. The liberated iodine was then immediately titrated with a standardized 0.10 mol L^{-1} sodium thiosulfate (Na₂S₂O₃) solution, using a 1.0% (w/v) starch solution as the indicator. Thiosulfate consumption was converted into dissolved ozone concentration based on reaction stoichiometry. All titrations were performed immediately after each experiment to estimate the dissolved ozone available during the aging processes. 45,47

2.4. Factorial Design. A 2^3 full factorial design with a central point was conducted in ultrapure water. This design allowed optimization of the O_3/H_2O_2 dose and reaction time,

maximizing the ΔTOC response attributable to MP aging. 26,48,49 The experimental design included three independent variables: H_2O_2 concentration (mg L⁻¹), O_3 concentration (mg L⁻¹), and reaction time (min). The design consisted of eight factorial points and a triplicate of the central point, for a total of 11 experimental runs performed in randomized order. TOC was measured for each experimental run. The variable ranges were as follows: H_2O_2 , 30.00–100.00 mg L^{-1} , O_3 , 34.00–52.00 mg L^{-1} ; and reaction time, 10–110 min (Tables S1 and S3, see Supporting Information). To quantify the extent of microplastic degradation, TOC was monitored throughout the ozonation process. Before each experiment, the TOC_{initial} was determined at time zero; after each run, the final TOC_{final} was measured. This metric allowed for the quantification of organic byproduct release resulting from the interaction between ozonation and PE-MPs, thereby providing a direct measure of the degree of aging.

2.5. Characterization of Degraded Microplastics. The chemical and physical properties of the PE-MPs were investigated. Chemical changes were initially assessed by Fourier transform infrared spectroscopy (FTIR) using a PerkinElmer spectrophotometer. For this analysis, potassium bromide (KBr) pellets containing PE-MPs samples were prepared, and spectra were acquired in the range of 4000 to 450 cm^{-1.35} Based on the chemical insights obtained by FTIR, the surface morphology of the PE-MPs samples was examined using a JSM-6380LV JEOL Scanning Electron Microscope (SEM).

The thermal stability of PE-MPs was analyzed by thermogravimetric analysis (TGA) using a TGA-Q50 V20 instrument. TGA monitors weight loss as a function of temperature, providing information on the decomposition behavior of the material. 50

2.6. Toxicity Tests. Toxicity tests on *A. salina* were performed following previous studies, as this organism is widely used in ecotoxicological assessments. ^{27,28,51} *A. salina* cysts were hatched in an artificial saline solution prepared with sea salt at a concentration of 30.00 g L⁻¹, with a pH of 8.00–9.00. The hatching process was conducted under controlled conditions, including constant aeration, a temperature of 28.00 \pm 2.00 °C, and a photoperiod of 16 h light/8 h dark for 48 h. The saline solution was used exclusively for *A. salina* cyst hatching and as the exposure medium during the bioassays; it was not the ozonation treatment matrix.

Each test was conducted in duplicate, with each replicate consisting of 10 larvae exposed in a 3.00 mL well within a Petri dish. 26,52,53 The assays were carried out with the leachate containing microplastics both before and after the aging processes. The assays used unfiltered whole suspensions (particles + leachates). The tests were performed over a 24 h period, during which the organisms were exposed to different concentrations of the degraded samples. The positive control (potassium dichromate, K₂Cr₂O₇, 0.1%) was included to verify test sensitivity. 54,55 The negative control (saline solution) was used for hatching and maintaining the organisms and was included in all assays. 27,51 Toxic effects such as reduced mobility, erratic swimming behavior, and mortality were carefully observed. Dead larvae were counted at the end of the exposure period, and the median lethal concentrations (LC_{50}) were calculated based on five serial dilutions of the test samples (100%, 75%, 50%, 25%, and 12.5%, v/v).

For the toxicity assays with *Artemia sp.*, three experimental conditions were prepared: post-UASB reactor effluent, without

the addition of microplastics (SW); post-UASB reactor effluent enriched with PE-MPs, not subjected to oxidative treatment (SW+MPs); and post-UASB reactor effluent enriched with PE-MPs and subsequently treated with hydrogen peroxide and ozone (O_3/H_2O_2) . The evaluation of these samples enabled analysis of the effect of adding MPs to the matrix and the determination of the ideal conditions for aging MPs.

To further classify the samples, toxicological units (TUs) were calculated using eq 1, which relates LC_{50} values to toxicity scoring systems. This classification was performed according to guidelines, ⁵⁶ allowing for a standardized evaluation of the environmental risk posed by the degraded microplastics. These tests provided critical insights into the potential ecotoxicological impacts of microplastic aging products on aquatic ecosystems.

$$TU = \left(\frac{1}{LC50}\right) x100 \tag{1}$$

2.7. Statistical Analysis. All statistical analyses were performed at a significant level of $\alpha=0.05$. For oxidative aging experiments, a 2^3 factorial design with three central-point replicates was analyzed using Statistica 12 (StatSoft, Tulsa, USA). A first-order polynomial model with two-factor interaction was fitted to predict the ΔTOC response, and model adequacy was supported by ANOVA ($R^2=0.9668$; adjusted $R^2=0.9170$), and residual analysis (Figure S3 - S4; Tables S4 - S5 see Supporting Information).

For A. salina bioassays, the LC_{50} and 95% confidence interval (CI) were estimated by Probit regression (StatPlus Mac, AnalystSoft version 8), ^{56,57} and model fit was evaluated by Pearson's chi-squared test. Toxicity comparisons were based on the overlap of 95% confidence intervals.

3. RESULTS AND DISCUSSION

3.1. Design of Experiments. In complex effluents, reactive oxygen species (ROS), such as hydroxyl radicals (HO•) generated during AOPs, can be consumed by reducing species, competitive ions, dissolved organic matter, and turbidity, thereby decreasing process efficiency. This transformation of effluent constituents, such as carbonates and nitrogenous compounds, into new potentially more toxic species represents a significant challenge. The ozonation of pharmaceuticals in real effluents has already demonstrated that satisfactory degradation can be achieved at near-neutral pH, eliminating the need for costly chemical adjustments. 27,28

Ozone reactions in aqueous media proceed through two main pathways: (i) a direct molecular ozone (O_3) attack, which is a selective reaction favored in acidic media, and (ii) an indirect oxidation by HO^{\bullet} , which is a more powerful and nonselective pathway favored at neutral pH. The indirect route is primarily initiated by the reaction between ozone and hydroxide ions (OH^-) , and since the concentration of these ions increases with pH, the decomposition of ozone and the subsequent generation of radicals are accelerated under neutral conditions. 58,59

Preliminary experiments were conducted at acidic, neutral, and basic pH, combining the O_3 and O_3/H_2O_2 process (Table S2, see Supporting Information). The difference in TOC between experiments under acidic and neutral conditions was only 0.02 mg L^{-1} . This observation is supported by studies suggesting that small variations in TOC may arise from the inherent limitations of quantification methods, particularly in

samples with low concentrations of dissolved organic carbon, making it unlikely that such variations reflect actual differences in the degradation process. ⁶⁰ Considering this minimal impact, together with the practical limitations and significant costs associated with large-scale pH adjustment, ^{61–63} the decision was made to operate at the natural pH. The similar pH values between ultrapure water and the effluent ensured the comparability of results.

The model shows that the average rate of ΔTOC increase occurs during the initial phase (10–60 min), after which it decelerates in the later phase (60–110 min). This observed slowdown is likely attributable to two concurrent phenomena. First, the initial, faster phase may correspond to the oxidative attack on the most labile sites of the polymer, such as defect structures or amorphous regions, leaving behind a more chemically resistant (recalcitrant) polymer surface for the later stages of the reaction. Second, as degradation proceeds, the soluble organic byproducts released into the solution can themselves act as important scavengers of hydroxyl radicals, competing with the solid PE-MPs for available oxidants and thereby slowing the overall degradation rate. S1

The experimental results of microplastic aging via ozone and hydrogen peroxide are summarized in Table 2.

Table 2. 2³ Factorial Design with the Results Obtained with the Total Carbon Analyzer

experiment		$O_3 (mg L^{-1})$	time (min)	$\Delta TOC \pmod{L^{-1}}$
4	100.00	52.00	10	0.86
8	100.00	52.00	110	1.04
3	30.00	52.00	10	0.23
7	30.00	52.00	110	0.24
11 (C)	65.00	43.00	60	0.51
10 (C)	65.00	43.00	60	0.40
1	30.00	34.00	10	0.21
6	100.00	34.00	110	0.34
2	100.00	34.00	10	0.33
5	30.00	34.00	110	0.30
9 (C)	65.00	43.00	60	0.34

Among the tested conditions, sample 8 exhibited the highest ΔTOC , reaching 1.04 mg L⁻¹ with 100.00 mg L⁻¹ H₂O₂, 52.00 mg L⁻¹ O₃, and a reaction time of 110 min. This outcome is consistent with the maximal oxidant dosing and prolonged residence time applied in run.⁶⁴ The ROS generated in the O₃/H₂O₂ process attacks the polymer network, causing structural modifications.³⁶ Prolonged exposure time is critical, as it allows this radical attack to propagate, leading to polymer chain scission and an increased presence of oxygen-containing functionalities on the surface.³⁷

In contrast, the central point reactions, which employed intermediate levels of H_2O_2 (65.00 mg L^{-1}), O_3 (43.00 mg L^{-1}), and reaction time (60 min), exhibited lower ΔTOC values (ranging from 0.34 to 0.51 mg L^{-1}). Similarly, sample 1, which applied the lowest levels of H_2O_2 (30.00 mg L^{-1}), O_3 (34.00 mg L^{-1}), and reaction time (10 min), yielded the lowest ΔTOC (0.21 mg L^{-1}).

Hydroxyl radical attack on polyethylene primarily occurs through hydrogen abstraction from C–H bonds, leading to the formation of alkyl radicals. These radicals subsequently react with oxygen to form hydroperoxide groups, which decompose into carbonyls and alcohols. This process leads to the oxidation of polymer chains and the formation of products including aldehydes, ketones, and carboxylic acids, which contribute to the measured $\Delta TOC.^{35}$

Although scission of the polymer chain occurs, the complete degradation of PE-MPs is a complex process influenced by factors such as the presence of unsaturated bonds and the stability of peroxyl radicals formed during oxidation. Therefore, the combination of $\rm H_2O_2$ and $\rm O_3$ at higher concentrations and over extended periods is effective for MPs aging, promoting structural alterations that lead to the conversion of the polymer into soluble products. 36,37

The results of the statistical analysis for the factorial design are shown in Figures 2 and 3. The Pareto chart (Figure 2A) highlights the influence of the tested variables on the ΔTOC response, where the red line indicates the threshold for statistical significance (p = 0.05). The ANOVA (Table S4, see Supporting Information) of the ΔTOC response yielded an R^2 of 0.96681 and an adjusted R^2 of 0.91702 (MS residual = 0.0060699). The H_2O_2 concentration (p = 0.001956), O_3

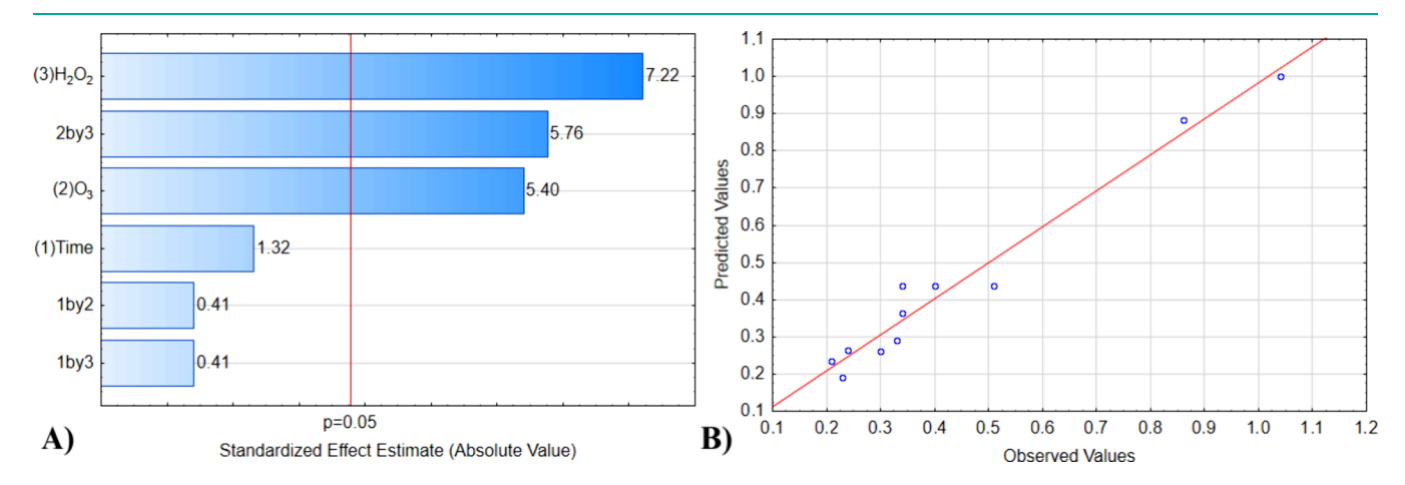


Figure 2. Statistical analysis of the factorial DOE for PE-MP aging (response ΔTOC , mg L⁻¹). (A) Pareto chart of standardized effects on ΔTOC with the significance threshold (red line, p = 0.05). Positive bars indicate factors that increase ΔTOC ; H₂O₂, O₃, and the H₂O₂ × O₃ interaction are statistically significant. (B) Predicted vs observed ΔTOC values (normal probability/residuals) for the fitted polynomial model. Model statistics: $R^2 = 0.9668$, adjusted $R^2 = 0.9170$, and MS residual = 0.00607.

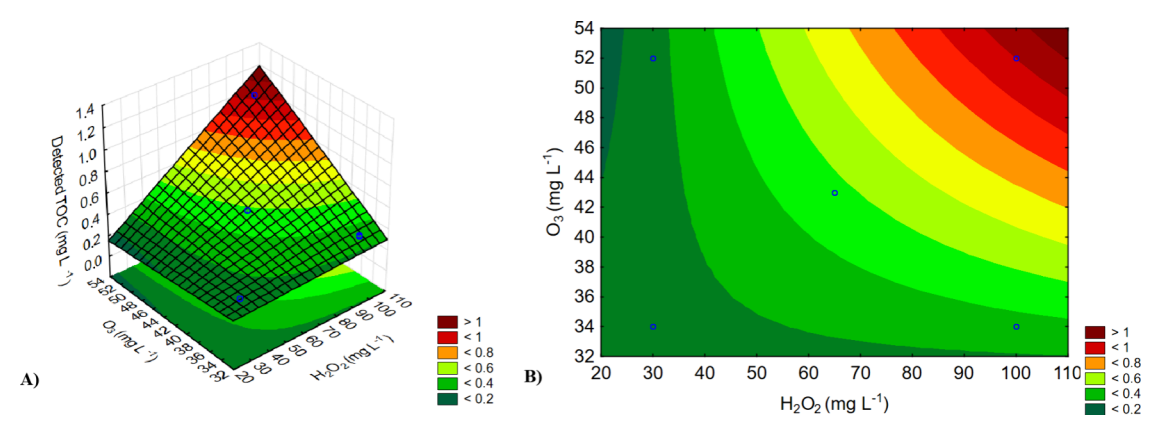


Figure 3. Response surface and contour plots for predicted ΔTOC (mg L^{-1}) as a function of H_2O_2 (mg L^{-1}) and O_3 (mg L^{-1}) from the factorial design. (a) 3D response surface showing the predicted ΔTOC . (b) 2D contour plot with the optimal region (red) where predicted $\Delta TOC > 0.80$ mg L^{-1} . Optimal operating point identified by DOE: 100.0 mg L^{-1} H_2O_2 and 52.0 mg L^{-1} O_3 .

concentration (p = 0.005691), and the $H_2O_2 \times O_3$ interaction (p = 0.004498) were all statistically significant.

Among the significant variables, H_2O_2 had the most pronounced effect, reaffirming its critical role as a key oxidizing agent in AOPs. When combined with O_3 , H_2O_2 facilitates the generation of HO^{\bullet} . Ozone itself was also a statistically significant factor, emphasizing its dual role as a direct oxidant and a catalyst for radical formation. The $H_2O_2 \times O_3$ interaction was also substantial, highlighting a positive synergistic relationship between these two agents, where their combined action exceeds the sum of their individual contributions. This synergy, indicated by the result observed in sample 8, is well established in the literature and occurs when the hydroperoxide anion (HO_2^{-}) , the conjugate base of H_2O_2 , initiates the rapid decomposition of ozone into HO^{\bullet} . 33,68

Experiments with O_3 ($H_2O_2 = 0 \text{ mg L}^{-1}$) were carried out to provide a reference for the oxidative performance of ozone alone in the same matrix and reactor configuration, Table S2 (see Supporting Information). For a reaction time of 110 min, the Δ TOC values obtained were 0.49 mg L⁻¹ at 34 mg O₃ L⁻¹, 0.56 mg L^{-1} at 43 mg O_3 L⁻¹, and 0.76 mg L^{-1} at 52 mg O_3 L⁻¹. These results offer a matrix-specific benchmark for comparison with the combined O₃/H₂O₂ treatments mapped by the DOE. In addition to the O₃ baseline runs, exploratory trials were performed at fixed ozone (43 mg L⁻¹) while varying H_2O_2 (30, 65, and 100 mg L^{-1}), which produced ΔTOC of 0.48, 0.76, and 1.12 mg L^{-1} , respectively. Finally, a pH screen at $O_3 = 43 \text{ mg L}^{-1}$ and $H_2O_2 = 65 \text{ mg L}^{-1}$ showed $\Delta TOC =$ 0.78 mg L⁻¹ at pH 3 and 0.76 mg L⁻¹ at pH 7 (Δ = 0.02 mg L⁻¹). Given the small pH effect observed and because operation at neutral pH better represents the UASB effluent matrix, pH was not controlled in the DOE; furthermore, pH adjustment at the treatment scale would entail additional reagent use and operational cost.

The Pareto chart (Figure 2A) demonstrates that H_2O_2 concentration has a positive effect on the ΔTOC response, revealing a synergistic relationship. This result indicates that higher concentrations of H_2O_2 promote the microplastic aging process. However, it is crucial to note that excessive dosage acts as a limiting factor due to its capacity to scavenge hydroxyl radicals (HO^{\bullet}), a mechanism extensively documented in the literature, as by Pipolo et al. ⁶⁹ While higher doses of H_2O_2 increase HO^{\bullet} generation, excessive concentrations can lead to scavenging effects, where H_2O_2 reacts with existing hydroxyl

radicals to form less reactive hydroperoxyl radicals $(HO_2^{\bullet})^{,40}$. The variable Time was not significant for PE-MPs aging efficiency. As shown in the chart, the main effect of Time was not statistically significant. Similarly, interactions involving time, such as the $H_2O_2 \times Time$ and $O_3 \times Time$ interactions, were also not important, which is consistent with other studies. ²⁸

As indicated by the plot of experimentally observed values versus those predicted by the model (Figure 2B), the statistical model showed a good fit. The R² value for the detected TOC was 0.9668, indicating a good distribution of the data points along the regression line and a low level of residuals. Further validation is provided by the diagnostic plots in the Supporting Information, which include a standard probability plot of raw residuals (Figure S3) and a studentized-deleted residuals plot (Figure S4), confirming the model's statistical validity.⁷⁰

The response surface plots (Figure 3A) reveal the synergistic effects of H_2O_2 and O_3 concentrations on ΔTOC . The highest ΔTOC value (>0.80 mg L^{-1}) was observed in a critical region (highlighted in red) at the maximum concentrations of both oxidants ($H_2O_2=100.00$ mg L^{-1} ; $O_3=52.00$ mg L^{-1}), highlighting the superior generation of HO^{\bullet} under these conditions. The contour plot highlights (Figure 3B) how this combination significantly enhances aging, as the curved gradients confirm that the interaction between the oxidants is more effective than their isolated effects.

3.2. Characterization of Degraded Polyethylene **Microplastics.** The FTIR spectra illustrating the degradation of PE-MPs after 110 min of treatment are presented in Figure 4. These spectra showcase the effects of the combined oxidative treatment (52.00 mg L⁻¹ O₃ and 100.00 mg L⁻¹ H_2O_2) on PE samples in both water and effluent matrices, revealing important insights into the chemical changes that occurred during the aging process. All spectra display the characteristic peaks of the C-H sp³ bond, which are distinctly observed at 2918 cm⁻¹ and 2848 cm⁻¹.³⁷ Consistent with the fundamental structure of polyethylene, these peaks represent the C-H stretching vibrations within the polymer chains. Additional peaks at 1467 cm⁻¹ and 1371 cm⁻¹ are attributed to the bending vibrations of methylene $(-CH_2-)$, while the peak at 719 cm⁻¹ corresponds to a planar asymmetric angular deformation associated with four or more CH2 groups in an open-chain configuration.

In the spectra of the degraded PE-MPs, new chemical features emerge, providing evidence of oxidation. Notably, a

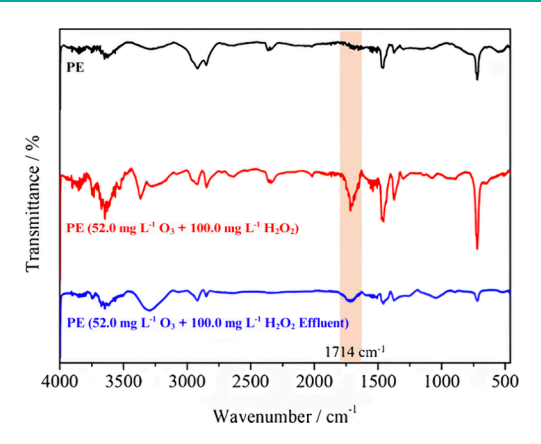


Figure 4. FTIR spectra of polyethylene (PE) samples: black for virgin PE (untreated), red for PE aged under O_3/H_2O_2 in ultrapure water (52.0 mg L^{-1} O_3 and 100.0 mg L^{-1} H_2O_2 for 110 min), and blue for PE aged under the same O_3/H_2O_2 condition in UASB effluent (110 min).

new peak appears at 1714 cm⁻¹, which is attributed to the presence of carbonyl groups (C = O). This observation is consistent with previous studies that reported the formation of carbonyl compounds during the oxidative degradation of polyethylene.^{29,35,36} Additionally, a broad absorption band between 3400 cm⁻¹ and 3600 cm⁻¹ is attributed to the O–H bond in alcohol groups. These peaks indicate the formation of hydroxyl functionalities during the reaction, likely due to the interaction of alkyl radicals with reactive oxygen species.^{35,36} The presence of these O–H groups suggests that the oxidative process introduced functional groups such as alcohols and hydroperoxides onto the polymer surface.⁷²

These hydroxyl and carbonyl functionalities not only alter the chemical composition of PE-MPs but also create active sites on the polymer surface. This phenomenon facilitates subsequent oxidation, promoting the further breakdown of the polymer chains. The broad absorption in the 3400–3600 cm⁻¹ range may also indicate the presence of hydroperoxides, which are intermediates in the degradation process and play a critical role in the generation of functional groups such as

ketones.³⁷ These chemical transformations highlight the complexity of the oxidative degradation mechanism and the potential for these processes to produce a variety of oxygencontaining species.⁷³

Following the FTIR analysis, thermogravimetric analysis (TGA) was used to examine the thermal stability of the samples. The TGA curves (Figure 5A) revealed a similar decomposition pattern among the analyzed PE-MPs samples, characterized by a progressive increase in the onset decomposition temperature (T $_{\rm onset}$). For the untreated PE, the T $_{\rm onset}$ was recorded at 436.18 °C. In contrast, PE-MPs aged in ultrapure water reached 442.88 °C, while PE aged in the UASB effluent showed the highest value at 449.35 °C. A similar trend was observed in the DTG curves (Figure 5B), where the temperature of maximum decomposition rate ($T_{\rm max}$) increased from 471.37 °C (untreated PE-MPs) to 473.51 °C (treated in water) and 479.16 °C (treated in effluent).

This apparent increase in thermal stability is a critical and somewhat counterintuitive finding. At the molecular scale, recent first-principles work shows that initial H-abstraction generates alkyl radicals that capture O_2 to form peroxy and hydroperoxide intermediates; the decomposition of these species (including hydroxyl-radical mediated channels) can yield both chain-cleaving products (e.g., ketones) and secondary radical species that propagate reactions or enable radical—radical coupling.⁷⁴ The conventional mechanism for oxidative degradation of plastics involves the formation of reactive radicals that promote chain scission, leading to the deterioration of polymer chains and, consequently, a reduction in thermal stability, a behavior consistently reported in the literature for oxidized polyethylene and other polyolefins.^{74,75}

Instead, the results observed here suggest the predominance of more complex and competing mechanisms. One plausible explanation is that the treatment induced polymer cross-linking within the bulk material. While this study focuses on polyethylene, similar behavior has been observed in other polymeric systems. For example, a study on polybenzoxazines reported that the incorporation of hydroxyl groups significantly increased thermal stability, not because of the groups themselves, but due to their ability to act as additional cross-

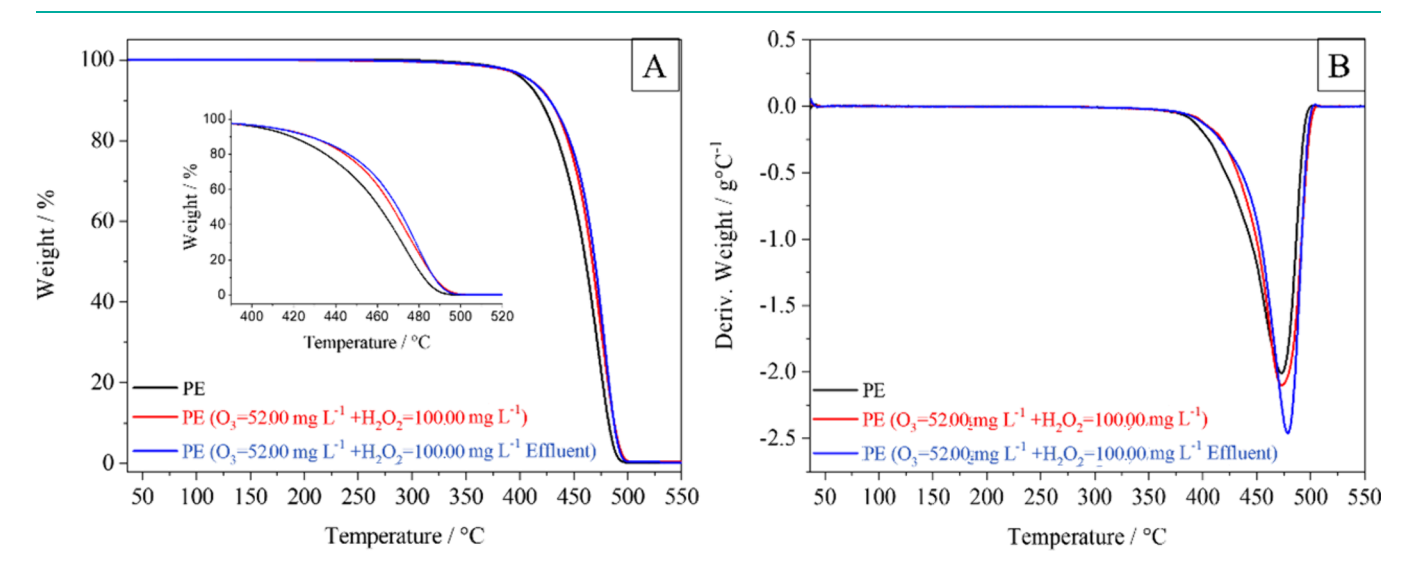


Figure 5. Thermogravimetric analysis of PE samples. (A) TGA thermograms (mass% vs temperature) for virgin PE and PE aged under O_3/H_2O_2 in ultrapure water and in UASB effluent (treated with 52.0 mg L^{-1} O_3 and 100.0 mg L^{-1} H_2O_2 for 110 min). (B) Corresponding DTG (derivative) curves (rate of mass loss vs temperature).

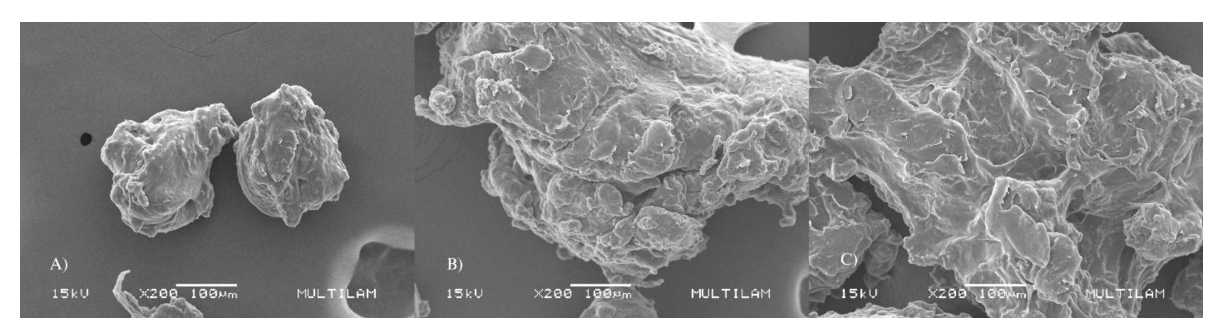


Figure 6. Representative SEM micrographs of PE-MPs: (A) pristine PE (untreated), (B) PE after oxidative aging under O_3/H_2O_2 in ultrapure water (optimal DOE condition being $100 \text{ mg L}^{-1} \text{ H}_2O_2$ and $52 \text{ mg L}^{-1} \text{ O}_3$ for 110 min), and (C) PE after oxidative aging under identical O_3/H_2O_2 conditions applied in post-UASB effluent.

linking sites and to establish a dense intermolecular hydrogenbonding network. Such condensation, cross-linking, or dense hydrogen-bonding networks at or near the polymer surface can locally increase thermal transition temperatures and char formation. This provides an experimental basis for higher apparent $T_{\rm onset}$ and $T_{\rm max}$ values, even while other fractions of the polymer are degraded.

Another mechanism that may have contributed is the preferential oxidation and solubilization of low-molecular-weight (LMW) fractions, such as oligomers and additives. The observed increase in total organic carbon (TOC) in the aqueous phase suggests that such LMW species were effectively removed during the treatment.

Thus, rather than contradicting the typical degradation pattern, these findings reveal a unique selectivity and structural reorganization promoted by the ${\rm O_3/H_2O_2}$ process. By simultaneously fostering cross-linking reactions and removing thermolabile fractions, this advanced oxidation approach directs the aging of PE-MPs toward a more thermally resilient and structurally modified state. These insights reinforce the potential of AOPs as a potent and selective tool for microplastic remediation, especially in complex environmental matrices such as UASB effluents. 74,75

To complement the chemical and thermal characterization, analysis of the surface morphology via SEM provides additional insight into the extent of microplastic aging. SEM examination is crucial for understanding the physical changes that microplastics undergo during oxidative degradation. As shown in Figure 6A, the surface of virgin PE-MPs is characterized by a smooth, nonporous, and relatively uniform texture. After 110 min of ozonation treatment, however, significant morphological changes become evident (Figure 6B). The previously smooth surface now exhibits visible pits, fissures, and fragments, highlighting the physical degradation caused by the ozonation process. These surface characteristics are consistent with previous studies, which report that oxidative attack on the polymer matrix generates pits and rough textures due to chain scission and the disruption of the polymer's structural integrity.³⁷ In other studies, prolonged ozonation (extending up to 180 min) exacerbates these changes. Features such as cracks and carbonyl-rich voids become more prominent as ozone and reactive intermediates penetrate deeper into the microplastic matrix, gradually oxidizing the surface layers."

These physical changes are accompanied by chemical changes, as the introduction of oxygen-containing functional groups further modifies the surface properties of the microplastics. Increased surface roughness, in turn, enhances the

adsorption capacity of the microplastics, allowing for greater interaction with reactive oxygen species and other environmental contaminants. This dual transformation, chemical and physical, demonstrates the profound impact of ozonation on PE-MPs, not only degrading the polymer matrix but also altering its surface chemistry. 35

Furthermore, comparison of SEM images of samples degraded in deionized water and wastewater reveals similar patterns of cracks, fissures, and surface roughness (Figure 6B and Figure 6C). This suggests that under identical experimental conditions 52.00 mg L^{-1} O_3 , 100.00 mg L^{-1} H_2O_2 , and equivalent reaction times), oxidative degradation occurs consistently, regardless of the aqueous medium. The presence of carbonyl-rich features in both cases confirms the uniformity of the degradation process.

Nasrabadi et al. (2025) demonstrated that the ozonation of smaller polystyrene microplastics (\approx 3.3 μ m) resulted in only a slight change in the mean particle size when analyzed by DLS, whereas the most pronounced modifications occurred at the surface, including an increased carbonyl index, surface cracking, porosity, and changes in surface charge. Recent reviews highlight the use of SEM, FTIR, and TGA as key tools to assess, respectively, the morphological, chemical, and thermal properties of microplastics. Our results emphasize the effectiveness of AOPs not only in accelerating the aging of MPs but also in promoting alterations in their chemical and physical properties, which may have significant implications for their environmental interactions and potential remediation strategies.

Although the ${\rm O_3/H_2O_2}$ system proved effective, other AOPs, such as UV/O₃ or photo-Fenton processes, may provide alternative pathways for MP aging. For example, the inclusion of UV light can enhance radical generation but introduces additional energy costs and challenges related to water turbidity, which is particularly relevant for UASB effluents. Therefore, an environmental remediation strategy should integrate AOPs with source reduction policies and efficient physical removal technologies to effectively address the challenge of microplastic contamination.

3.3. lodometry. The average value of residual ozone for the treatment of microplastics in deionized water was 4.50 mg $\rm L^{-1}$, while for treatment in effluent, the value was 2.80 mg $\rm L^{-1}$. The permitted mean of residual ozone in drinking water is 2.00 to 5.00 mg $\rm L^{-1}$, according to the World Health Organization's Guidelines for Drinking-Water Quality, meaning the values found in this study are within the required standards. ⁸¹

3.4. Assessment of Acute Toxicity in A. salina. A. salina is widely used in these assays due to its rapid egg hatching,

minimal storage requirements for reagents, and ease of handling during test execution. For both toxicity assays, three samples were evaluated. Toxicity assays were performed on three samples, as defined in the Methods section: the raw effluent (SW), the effluent with microplastics (SW+MPs), and the effluent with microplastics after O_3/H_2O_2 treatment. The assays used unfiltered whole suspensions (particles + leachates); therefore, observed effects represent combined physical and chemical influences, whereas ΔTOC refers only to the filtered, dissolved fraction. The results, including toxicity units (TU) and their classifications, are shown in Table 3.

Table 3. LC₅₀ and TU Values for the Effluent (SW), the Solution Containing Microplastics (SW+MPs), and the Samples Treated with Ozonation $(O_3/H_2O_2)^a$

sample	lethal concentration, LC_{50} (%)	toxic unit (TU)	toxicity classification
SW	91.97	1.09	acutely toxic
SW+MPs	87.42	1.14	acutely toxic
O_3/H_2O_2	N/C	N/C	nontoxic

 $^{\alpha}$ N/C = not calculated. For the O_3/H_2O_2 -treated sample, no mortality was observed at any of the concentrations tested. The evaluated samples were treated under the optimized condition.

Using TU values, samples were categorized based on the toxicity classification system detailed in Table S6 (see Supporting Information). According to this system, both the effluent sample without microplastics (SW) and the effluent containing microplastics (SW + MPs) demonstrated acute toxicity, with TU values ranging from 1.0 to 10.0. These results indicate that both untreated samples pose a significant toxicological risk.

The LC₅₀ for the SW was determined to be 91.97% with a narrow 95% confidence interval (95% CI: 85.71–98.74%), indicating a consistent toxic response. Upon the addition of microplastics (SW+MPs), the LC₅₀ was 87.42%. Although this value is numerically lower, suggesting higher toxicity, it is accompanied by a much wider confidence interval (95% CI: 24.49–312.05%). This wide confidence interval for the SW +MPs sample, derived from the standard error of the Log₁₀[LC₅₀] in the probit analysis, indicates that the presence of microplastics introduced significant variability to the system's toxic response. While the overlapping confidence intervals prevent a claim of a statistically significant difference in this acute test, it is noteworthy that the mean toxicity did trend higher with the addition of MPs. This observation supports the rationale for intervention.

In contrast, the O_3/H_2O_2 treated effluent produced no observable mortality at any dilution (100–12.5% v/v); therefore, the LC_{50} is not determinable. For classification purposes, a TU value of 0.00 was assigned to this sample, which, according to the toxicity system, confirms the absence of acute toxicity.

The absence of acute toxicity in the treated effluent is attributed to the efficient aging of the microplastic particles and the subsequent conversion of potentially harmful intermediates into less toxic or nontoxic byproducts. The most frequently reported intermediates in the literature for AOP-driven microplastic degradation are benzoic acid, carboxylic acids, formic acid, methyl benzaldehyde, and acetophenone. The ozonation process is driven by ROS, such as HO•, which initiate oxidative reactions in PE-

MPs. 35 During prolonged ozonation, these intermediates are subsequently mineralized into CO_2 and water, significantly reducing their environmental impact. These findings highlight the effectiveness of AOPs in mitigating the acute toxicity of effluents containing MPs, while promoting the degradation of hazardous intermediates into benign end products. This work further underscores the potential of ozonation as a promising strategy to reduce the ecological risks posed by MPs and other pollutants in wastewater.

4. CONCLUSION

The application of the ${\rm O_3/H_2O_2}$ advanced oxidation process successfully induced the aging of PE-MPs within a real UASB reactor effluent matrix. The treatment caused significant structural modifications, including surface erosion, formation of carbonyl groups, and the release of soluble organic carbon. Notably, these alterations led to an unexpected increase in the polymer's apparent thermal stability, with the $T_{\rm onset}$ rising from 436.18 to 449.35 °C. This result suggests the removal of low-molecular-weight fractions, corroborated by TOC data, and structural rearrangements such as bulk polymer cross-linking.

The treated effluent showed no acute toxicity to A. salina, and the residual ozone concentration (2.80 mg $\rm L^{-1}$) complied with regulatory standards. Thus, the central contribution of this work was to demonstrate the potential of an advanced oxidation process by aging a polymer within a complex effluent matrix in an environmentally safe manner. The combined demonstration of efficacy and safety under nonidealized conditions represents an important step toward the practical application of the $\rm O_3/H_2O_2$ system for mitigating microplastic pollution in existing treatment plants.

ASSOCIATED CONTENT

Supporting Information

The Supporting Information is available free of charge at https://pubs.acs.org/doi/10.1021/acsestwater.5c00773.

Overview of additional experimental results, factorial design data, toxicity classification, and images of the ozonation setup and process (PDF)

AUTHOR INFORMATION

Corresponding Author

Amilcar M. Junior — Institute of Chemistry, Federal University of Rio Grande do Norte, Natal, RN 59078-970, Brazil; orcid.org/0000-0002-4632-4647; Email: machulekjr@gmail.com, amilcar.machulek@ufrn.br

Authors

Diego A. S. Brito — College of Engineering, Architecture and Urbanism and Geography, Federal University of Mato Grosso do Sul, Campo Grande, MS 79070-900, Brazil

Thalita F. Silva – São Carlos Institute of Chemistry, University of São Paulo, São Carlos, SP 13566-590, Brazil

Priscila S. Cavalheri – Institute of Physics, Federal University of Mato Grosso do Sul, Campo Grande, MS 79070-900, Brazil

Antonio K. Canatto – College of Engineering, Architecture and Urbanism and Geography, Federal University of Mato Grosso do Sul, Campo Grande, MS 79070-900, Brazil

Emmanuel S. C. Miguel – Institute of Physics, Federal University of Mato Grosso do Sul, Campo Grande, MS 79070-900, Brazil

- Fernando Jorge C. M. Filho Institute of Hydraulic Research, Federal University of Rio Grande do Sul, Porto Alegre, RS 90650-005, Brazil
- Lincoln C. S. Oliveira Institute of Chemistry, Federal University of Mato Grosso do Sul, Campo Grande, MS 79074-460, Brazil
- Gleison A. Casagrande Institute of Chemistry, Federal University of Mato Grosso do Sul, Campo Grande, MS 79074-460, Brazil

Complete contact information is available at: https://pubs.acs.org/10.1021/acsestwater.5c00773

Author Contributions

D.A.S.B.: conceptualization, data curation, formal analysis, investigation, methodology, and writing of the original draft. T.F.S. and P.S.C.: supervision, validation, visualization, and review and editing. A.K.C. and E.S.C.M.: visualization and review and editing. F.J.C.M.F.: conceptualization, visualization, and review and editing. L.C.S.O. and G.A.C.: review and editing. A.M.J.: supervision, conceptualization, formal analysis, investigation, methodology, validation, visualization, and review and editing. CRediT: Diego Aparecido Silva de Brito conceptualization, data curation, formal analysis, investigation, methodology, writing - original draft; Thalita F. da Silva supervision, validation, visualization, writing review & editing; Priscila Sabioni Cavalheri supervision, validation, visualization, writing - review & editing; Antonio Kaique Canatto visualization, writing - review & editing; Emmanuel Silva Côgo Miguel visualization, writing - review & editing; Fernando Jorge Correa Magalhães Filho conceptualization, visualization, writing - review & editing; Lincoln Carlos Silva de Oliveira writing - review & editing; Gleison Antônio Casagrande writing - review & editing; Amilcar Machulek Junior conceptualization, formal analysis, investigation, methodology, supervision, validation, visualization, writing - review & editing.

Funding

The Article Processing Charge for the publication of this research was funded by the Coordenacao de Aperfeicoamento de Pessoal de Nivel Superior (CAPES), Brazil (ROR identifier: 00x0ma614).

Notes

The authors declare no competing financial interest.

ACKNOWLEDGMENTS

The authors thank the following Brazilian funding agencies: Conselho Nacional de Desenvolvimento Científico e Tecnológico (CNPq), Coordenação de Aperfeiçoamento de Pessoal de Nível Superior (CAPES - Financing Code 001), and Fundação de Apoio ao Desenvolvimento do Ensino, Ciência e Tecnologia do Estado de Mato Grosso do Sul (FUNDECT).

REFERENCES

- (1) Borrelle, S. B.; Ringma, J.; Law, K. L.; Monnahan, C. C.; Lebreton, L.; McGivern, A.; Murphy, E.; Jambeck, J.; Leonard, G. H.; Hilleary, M. A.; Eriksen, M.; Possingham, H. P.; De Frond, H.; Gerber, L. R.; Polidoro, B.; Tahir, A.; Bernard, M.; Mallos, N.; Barnes, M.; Rochman, C. M. Predicted Growth in Plastic Waste Exceeds Efforts to Mitigate Plastic Pollution. *Science* (1979) **2020**, 369 (6510), 1515–1518.
- (2) Cao, J.; Xu, R.; Wang, F.; Geng, Y.; Xu, T.; Zhu, M.; Lv, H.; Xu, S.; Guo, M. Polyethylene Microplastics Trigger Cell Apoptosis and Inflammation via Inducing Oxidative Stress and Activation of the

- NLRP3 Inflammasome in Carp Gills. Fish Shellfish Immunol 2023, 132, 108470.
- (3) Yang, Q.; Peng, Y.; Wu, X.; Cao, X.; Zhang, P.; Liang, Z.; Zhang, J.; Zhang, Y.; Gao, P.; Fu, Y.; Liu, P.; Cao, Z.; Ding, T. Microplastics in Human Skeletal Tissues: Presence, Distribution and Health Implications. *Environ. Int.* **2025**, *196*, 109316.
- (4) Chakraborty, S.; Banerjee, M.; Jayaraman, G.; Rajeswari V, D. Evaluation of the Health Impacts and Deregulation of Signaling Pathways in Humans Induced by Microplastics. *Chemosphere* **2024**, *369*, 143881.
- (5) Ziajahromi, S.; Neale, P. A.; Rintoul, L.; Leusch, F. D. L. Wastewater Treatment Plants as a Pathway for Microplastics: Development of a New Approach to Sample Wastewater-Based Microplastics. *Water Res.* **2017**, *112*, 93–99.
- (6) Hajji, S.; Ben-Haddad, M.; Abelouah, M. R.; De-la-Torre, G. E.; Alla, A. A. Occurrence, Characteristics, and Removal of Microplastics in Wastewater Treatment Plants Located on the Moroccan Atlantic: The Case of Agadir Metropolis. *Science of The Total Environment* **2023**, *862*, 160815.
- (7) Bayo, J.; Olmos, S.; López-Castellanos, J. Microplastics in an Urban Wastewater Treatment Plant: The Influence of Physicochemical Parameters and Environmental Factors. *Chemosphere* **2020**, 238, 124593
- (8) Kole, P. J.; Löhr, A. J.; Van Belleghem, F.; Ragas, A. Wear and Tear of Tyres: A Stealthy Source of Microplastics in the Environment. *Int. J. Environ. Res. Public Health* **2017**, *14* (10), 1265.
- (9) Eriksen, M.; Mason, S.; Wilson, S.; Box, C.; Zellers, A.; Edwards, W.; Farley, H.; Amato, S. Microplastic Pollution in the Surface Waters of the Laurentian Great Lakes. *Mar. Pollut. Bull.* **2013**, 77 (1–2), 177–182.
- (10) Hernandez, E.; Nowack, B.; Mitrano, D. M. Polyester Textiles as a Source of Microplastics from Households: A Mechanistic Study to Understand Microfiber Release During Washing. *Environ. Sci. Technol.* **2017**, *51* (12), 7036–7046.
- (11) Napper, I. E.; Thompson, R. C. Release of Synthetic Microplastic Plastic Fibres from Domestic Washing Machines: Effects of Fabric Type and Washing Conditions. *Mar. Pollut. Bull.* **2016**, *112* (1–2), 39–45.
- (12) Akarsu, C.; Kumbur, H.; Gökdağ, K.; Kıdeys, A. E.; Sanchez-Vidal, A. Microplastics Composition and Load from Three Wastewater Treatment Plants Discharging into Mersin Bay, North Eastern Mediterranean Sea. *Mar. Pollut. Bull.* **2020**, *150*, 110776.
- (13) Murphy, F.; Ewins, C.; Carbonnier, F.; Quinn, B. Wastewater Treatment Works (WwTW) as a Source of Microplastics in the Aquatic Environment. *Environ. Sci. Technol.* **2016**, *50* (11), 5800–5808
- (14) Mintenig, S. M.; Int-Veen, I.; Löder, M. G. J.; Primpke, S.; Gerdts, G. Identification of Microplastic in Effluents of Waste Water Treatment Plants Using Focal Plane Array-Based Micro-Fourier-Transform Infrared Imaging. *Water Res.* **2017**, *108*, 365–372.
- (15) Gies, E. A.; LeNoble, J. L.; Noël, M.; Etemadifar, A.; Bishay, F.; Hall, E. R.; Ross, P. S. Retention of Microplastics in a Major Secondary Wastewater Treatment Plant in Vancouver, Canada. *Mar. Pollut. Bull.* **2018**, *133*, 553–561.
- (16) He, P.; Chen, L.; Shao, L.; Zhang, H.; Lü, F. Municipal Solid Waste (MSW) Landfill: A Source of Microplastics? -Evidence of Microplastics in Landfill Leachate. *Water Res.* **2019**, *159*, 38–45.
- (17) Gouveia, R.; Antunes, J.; Sobral, P.; Amaral, L. Microplastics from Wastewater Treatment Plants—Preliminary Data. *Proceedings of the International Conference on Microplastic Pollution in the Mediterranean Sea* **2018**, 53–57.
- (18) Cai, M.; Liu, M.; Hossain, K. B.; Wang, J.; Zhou, Y.; Yan, M.; Leung, K. M. Y. Current Status and Emerging Techniques for Sampling, Separating, and Identifying Microplastics in Freshwater Environments. *TrAC Trends in Analytical Chemistry* **2025**, *184*, 118151.
- (19) Wu, J.; Zhang, Y.; Tang, Y. Fragmentation of Microplastics in the Drinking Water Treatment Process - A Case Study in Yangtze

- River Region, China. Science of The Total Environment 2022, 806, 150545.
- (20) Volke-Sepúlveda, T.; Saucedo-Castañeda, G.; Gutiérrez-Rojas, M.; Manzur, A.; Favela-Torres, E. Thermally Treated Low Density Polyethylene Biodegradation by *Penicillium Pinophilum* and *Aspergillus Niger*. J. Appl. Polym. Sci. **2002**, 83 (2), 305–314.
- (21) Auta, H. S.; Emenike, C. U.; Fauziah, S. H. Screening of Bacillus Strains Isolated from Mangrove Ecosystems in Peninsular Malaysia for Microplastic Degradation. *Environ. Pollut.* **2017**, 231, 1552–1559.
- (22) Gozzi, F.; Sirés, I.; de Oliveira, S. C.; Machulek, A.; Brillas, E. Influence of Chelation on the Fenton-Based Electrochemical Degradation of Herbicide Tebuthiuron. *Chemosphere* **2018**, *199*, 709–717.
- (23) Luna, A. J.; Chiavone-Filho, O.; Machulek, A.; de Moraes, J. E. F.; Nascimento, C. A. O. Photo-Fenton Oxidation of Phenol and Organochlorides (2,4-DCP and 2,4-D) in Aqueous Alkaline Medium with High Chloride Concentration. *J. Environ. Manage* **2012**, *111*, 10–17.
- (24) Cavalheri, P. S.; Machado, B. S.; da Silva, T. F.; Rodrigues, J. P. B. G.; Gozzi, F.; Filho, F. J. C. M.; Cavalcante, R. P.; de Oliveira, S. C.; Junior, A. M. Optimization of a Combined System of Vertical Flow Constructed Wetland and Solar Photo-Fenton for Ketoprofen Removal in Sewage and Landfill Leachate. *Chemical Engineering Journal* 2023, 475, 146282.
- (25) Cavalheri, P. S.; Machado, B. S.; da Silva, T. F.; Warszawski de Oliveira, K. R.; Magalhães Filho, F. J. C.; Nazário, C. E.; Cavalcante, R. P.; de Oliveira, S. C.; Junior, A. M. Ketoprofen and Diclofenac Removal and Toxicity Abatement in a Real Scale Sewage Treatment Plant by Photo-Fenton Process with Design of Experiments. *J. Environ. Chem. Eng.* **2023**, *11* (5), 110699.
- (26) Antonio da Silva, D.; Cavalcante, R. P.; Cunha, R. F.; Machulek, A.; César de Oliveira, S. Optimization of Nimesulide Oxidation via a UV-ABC/H₂O₂ Treatment Process: Degradation Products, Ecotoxicological Effects, and Their Dependence on the Water Matrix. *Chemosphere* **2018**, 207, 457–468.
- (27) Cavalheri, P. S.; da Silva, T. F.; Miguel, E. da S. C.; Canatto, A. K.; Magalhães Filho, F. J. C.; Cavalcante, R. P.; de Oliveira, S. C.; Machulek Junior, A. Enhanced Degradation and Toxicity Reduction of Diclofenac and Ketoprofen Using UASB Reactor and O₃/H₂O₂ at Neutral pH. *Journal of Water Process Engineering* **2025**, 72, 107644.
- (28) Canatto, A. K.; da Silva, T. F.; dos Santos Machado, B.; Gozzi, F.; de Brito, D. A. S.; Nazário, C. E. D.; Filho, F. J. C. M.; Cavalheri, P. S.; de Oliveira, S. C.; Junior, A. M. Ozonation Process at Neutral pH Integrated with Anaerobic Treatment System to Methylparaben Removal. *Journal of Water Process Engineering* **2024**, *64*, 105741.
- (29) Gomes de Aragão Belé, T.; F. Neves, T.; Cristale, J.; Prediger, P.; Constapel, M.; F. Dantas, R. Oxidation of Microplastics by O₃ and O₃/H₂O₂: Surface Modification and Adsorption Capacity. *Journal of Water Process Engineering* **2021**, *41*, 102072.
- (30) Friedrich, L. C.; Zanta, C. L. d. P. e S.; Machulek, A., Jr; Silva, V. de O.; Quina, F. H. Interference of Inorganic Ions on Phenol Degradation by the Fenton Reaction. *Sci. Agric.* (*Piracicaba, Braz.*) **2012**, *69* (*6*), 347–351.
- (31) Teodoro, A.; Boncz, M. Á.; Júnior, A. M.; Paulo, P. L. Disinfection of Greywater Pre-Treated by Constructed Wetlands Using Photo-Fenton: Influence of pH on the Decay of Pseudomonas Aeruginosa. *J. Environ. Chem. Eng.* **2014**, 2 (2), 958–962.
- (32) Machulek, A.; et al. Application of Different Advanced Oxidation Processes for the Degradation of Organic Pollutants. In Organic Pollutants Monitoring, Risk and Treatment; InTech, 2013. DOI: 10.5772/53188
- (33) Poyatos, J. M.; Muñio, M. M.; Almecija, M. C.; Torres, J. C.; Hontoria, E.; Osorio, F. Advanced Oxidation Processes for Wastewater Treatment: State of the Art. *Water Air Soil Pollut* **2010**, 205 (1–4), 187–204.
- (34) Smith, L. M.; Aitken, H. M.; Coote, M. L. The Fate of the Peroxyl Radical in Autoxidation: How Does Polymer Degradation Really Occur? *Acc. Chem. Res.* **2018**, *51* (9), 2006–2013.

- (35) Zafar, R.; Park, S. Y.; Kim, C. G. Surface Modification of Polyethylene Microplastic Particles during the Aqueous-Phase Ozonation Process. *Environmental Engineering Research* **2021**, 26 (5), 200412–0.
- (36) Amelia, D.; Fathul Karamah, E.; Mahardika, M.; Syafri, E.; Mavinkere Rangappa, S.; Siengchin, S.; Asrofi, M. Effect of Advanced Oxidation Process for Chemical Structure Changes of Polyethylene Microplastics. *Mater. Today Proc.* **2022**, *52*, 2501–2504.
- (37) Hu, J.; Lim, F. Y.; Hu, J. Ozonation Facilitates the Aging and Mineralization of Polyethylene Microplastics from Water: Behavior, Mechanisms, and Pathways. *Science of The Total Environment* **2023**, *866*, 161290.
- (38) Singh, B.; Sharma, N. Mechanistic Implications of Plastic Degradation. *Polym. Degrad. Stab.* **2008**, 93 (3), 561–584.
- (39) Tian, L.; Kolvenbach, B.; Corvini, N.; Wang, S.; Tavanaie, N.; Wang, L.; Ma, Y.; Scheu, S.; Corvini, P. F.-X.; Ji, R. Mineralisation of 14C-Labelled Polystyrene Plastics by Penicillium Variabile after Ozonation Pre-Treatment. *N Biotechnol* **2017**, *38*, 101–105.
- (40) Yang, X.; Rosario-Ortiz, F. L.; Lei, Y.; Pan, Y.; Lei, X.; Westerhoff, P. Multiple Roles of Dissolved Organic Matter in Advanced Oxidation Processes. *Environ. Sci. Technol.* **2022**, *56* (16), 11111–11131.
- (41) Na, S.-H.; Kim, M.-J.; Kim, J.-T.; Jeong, S.; Lee, S.; Chung, J.; Kim, E.-J. Microplastic Removal in Conventional Drinking Water Treatment Processes: Performance, Mechanism, and Potential Risk. *Water Res.* **2021**, 202, 117417.
- (42) Ghobish, S. A.; Motti, C. A.; Bissember, A. C.; Vamvounis, G. Microplastics in the Marine Environment: Challenges and the Shift towards Sustainable Plastics and Plasticizers. *J. Hazard Mater.* **2025**, 491, 137945.
- (43) Lipps, W. C.; Braun-Howland, E. B.; Baxter, T. E. Standard Methods for the Examination of Water and Wastewater; American Public Health Association, 2023.
- (44) CONAMA no 357. Dispõe Sobre a Classificação Dos Corpos de Água e Diretrizes Ambientais Para o Seu Enquadramento, Bem Como Estabelece as Condições e Padrões de Lançamento de Efluentes, e Dá Outras Providências. Brasil, 2005.
- (45) Triandi Tjahjanto, R.; Galuh R, D.; Wardhani, S. Ozone Determination: A Comparison of Quantitative Analysis Methods. *J. Pure Appl. Chem. Res.* **2012**, *1* (1), 18–25.
- (46) Tsochatzis, E. D.; Gika, H.; Theodoridis, G.; Maragou, N.; Thomaidis, N.; Corredig, M. Microplastics and Nanoplastics: Exposure and Toxicological Effects Require Important Analysis Considerations. *Heliyon* **2024**, *10* (11), No. e32261.
- (47) Antonio da Silva, D.; Pereira Cavalcante, R.; Batista Barbosa, E.; Machulek Junior, A.; César de Oliveira, S.; Falcao Dantas, R. Combined AOP/GAC/AOP Systems for Secondary Effluent Polishing: Optimization, Toxicity and Disinfection. Sep Purif Technol. 2021, 263, 118415.
- (48) Cristale, J.; Ramos, D. D.; Dantas, R. F.; Machulek Junior, A.; Lacorte, S.; Sans, C.; Esplugas, S. Can. Activated Sludge Treatments and Advanced Oxidation Processes Remove Organophosphorus Flame Retardants? *Environ. Res.* **2016**, *144*, 11–18.
- (49) Gozzi, F.; Machulek, A.; Ferreira, V. S.; Osugi, M. E.; Santos, A. P. F.; Nogueira, J. A.; Dantas, R. F.; Esplugas, S.; de Oliveira, S. C. Investigation of Chlorimuron-Ethyl Degradation by Fenton, Photo-Fenton and Ozonation Processes. *Chemical Engineering Journal* **2012**, 210, 444–450.
- (50) Enyoh, C. E.; Ovuoraye, P. E.; Rabin, M. H.; Qingyue, W.; Tahir, M. A. Thermal Degradation Evaluation of Polyethylene Terephthalate Microplastics: Insights from Kinetics and Machine Learning Algorithms Using Non-Isoconversional TGA Data. *J. Environ. Chem. Eng.* **2024**, *12* (2), 111909.
- (51) Miguel, E. da S. C.; Machado, B. S.; Teles, A. P. S.; da Silva, T. F.; Magalhães Filho, F. J. C.; Cavalheri, P. S. Optimizing Sewage Treatment by UV/H₂O₂ Process and Vertical Flow Constructed Wetland Integration. *Journal of Water Process Engineering* **2024**, *64*, 105580.

- (52) da Silva, T. F.; Cavalcante, R. P.; Guelfi, D. R. V.; de Oliveira, S. C.; Casagrande, G. A.; Caires, A. R. L.; de Oliveira, F. F.; Gubiani, J. R.; Cardoso, J. C.; Machulek, A. Photo-Anodes Based on B-Doped TiO₂ for Photoelectrocatalytic Degradation of Propyphenazone: Identification of Intermediates, and Acute Toxicity Evaluation. *J. Environ. Chem. Eng.* **2022**, *10* (2), 107212.
- (53) de Melo da Silva, L.; Gozzi, F.; Sirés, I.; Brillas, E.; de Oliveira, S. C.; Machulek, A. Degradation of 4-Aminoantipyrine by Electro-Oxidation with a Boron-Doped Diamond Anode: Optimization by Central Composite Design, Oxidation Products and Toxicity. *Science of The Total Environment* **2018**, 631–632, 1079–1088.
- (54) Salay, G.; Lucarelli, N.; Gascón, T. M.; Carvalho, S. S. de; Veiga, G. R. L. da; Reis, B. da C. A. A.; Fonseca, F. L. A. Acute Toxicity Assays with the *Artemia Salina Model*: Assessment of Variables. *Alternatives to Laboratory Animals* **2024**, 52 (3), 142–148.
- (55) Meyer, B.; Ferrigni, N.; Putnam, J.; Jacobsen, L.; Nichols, D.; McLaughlin, J. Brine Shrimp: A Convenient General Bioassay for Active Plant Constituents. *Planta Med.* **1982**, *45* (05), 31–34.
- (56) Persoone, G.; Marsalek, B.; Blinova, I.; Törökne, A.; Zarina, D.; Manusadzianas, L.; Nalecz-Jawecki, G.; Tofan, L.; Stepanova, N.; Tothova, L.; Kolar, B. A Practical and User-friendly Toxicity Classification System with Microbiotests for Natural Waters and Wastewaters. *Environ. Toxicol* **2003**, *18* (6), 395–402.
- (57) Faria, R. S.; Silva, H. D.; Mello-Andrade, F.; Pires, W. C.; de Castro Pereira, F.; de Lima, A. P.; de Fátima Oliveira Santos, S.; Teixeira, T. M.; da Silva, P. F. F.; Naves, P. L. F.; Batista, A. A.; da Silva Oliveira, R. J.; Reis, R. M.; de Paula Silveira-Lacerda, E. Ruthenium(II)/Benzonitrile Complex Induces Cytotoxic Effect in Sarcoma-180 Cells by Caspase-Mediated and Tp53/P21-Mediated Apoptosis, with Moderate Brine Shrimp Toxicity. *Biol. Trace Elem Res.* 2020, 198 (2), 669–680.
- (58) Lovato, M. E.; Martín, C. A.; Cassano, A. E. A Reaction Kinetic Model for Ozone Decomposition in Aqueous Media Valid for Neutral and Acidic pH. *Chemical Engineering Journal* **2009**, *146* (3), 486–497.
- (59) Zhao, L.; Ma, W.; Lu, S.; Ma, J. Influencing Investigation of Metal Ions on Heterogeneous Catalytic Ozonation by Ceramic Honeycomb for the Degradation of Nitrobenzene in Aqueous Solution with Neutral pH. Sep Purif Technol. 2019, 210, 167–174.
- (60) Kim, J.-W.; Lee, H.-S.; Lim, H.-B.; Shin, H.-S. Identification of the Cause of the Difference among TOC Quantitative Methods According to the Water Sample Characteristics. *Science of The Total Environment* **2023**, 875, 162530.
- (61) Miralles-Cuevas, S.; Darowna, D.; Wanag, A.; Mozia, S.; Malato, S.; Oller, I. Comparison of UV/H_2O_2 , $UV/S_2O_8^{2-}$, Solar/Fe(II)/ H_2O_2 and Solar/Fe(II)/ $S_2O_8^{2-}$ at Pilot Plant Scale for the Elimination of Micro-Contaminants in Natural Water: An Economic Assessment. Chemical Engineering Journal **2017**, 310, 514–524.
- (62) Boczkaj, G.; Fernandes, A. Wastewater Treatment by Means of Advanced Oxidation Processes at Basic PH Conditions: A Review. *Chemical Engineering Journal* **2017**, 320, 608–633.
- (63) Munter, R.; Trapido, M.; Veressinina, Y.; Goi, A. Cost Effectiveness of Ozonation and AOPs for Aromatic Compound Removal from Water: A Preliminary Study. *Ozone Sci. Eng.* **2006**, 28 (5), 287–293.
- (64) Suzuki, H.; Yamagiwa, S.; Araki, S.; Yamamoto, H. Effects of Advanced Oxidation Processes on the Decomposition Properties of Organic Compounds with Different Molecular Structures in Water. *J. Water Resour Prot* **2016**, *08* (09), 823–834.
- (65) Zhang, X.; Fevre, M.; Jones, G. O.; Waymouth, R. M. Catalysis as an Enabling Science for Sustainable Polymers. *Chem. Rev.* **2018**, 118 (2), 839–885.
- (66) Tian, L.; Kolvenbach, B.; Corvini, N.; Wang, S.; Tavanaie, N.; Wang, L.; Ma, Y.; Scheu, S.; Corvini, P. F.-X.; Ji, R. Mineralisation of 14C-Labelled Polystyrene Plastics by Penicillium Variabile after Ozonation Pre-Treatment. N Biotechnol 2017, 38, 101–105.
- (67) Akmehmet Balcıoğlu, I.; Ötker, M. Treatment of Pharmaceutical Wastewater Containing Antibiotics by O₃ and O₃/H₂O₂ Processes. *Chemosphere* **2003**, *50* (1), 85–95.

- (68) Pipolo, M.; Gmurek, M.; Corceiro, V.; Costa, R.; Emília Quinta-Ferreira, M.; Ledakowicz, S.; Quinta-Ferreira, R. M.; Martins, R. C. Ozone-Based Technologies for Parabens Removal from Water: Toxicity Assessment. *Ozone Sci. Eng.* **2017**, *39* (4), 233–243.
- (69) Murrell, K. A.; Ghetu, C. C.; Dorman, F. L. The Combination of Spectroscopy, Microscopy, and Profilometry Methods for the Physical and Chemical Characterization of Environmentally Relevant Microplastics. *Analytical Methods* **2018**, *10* (40), 4909–4916.
- (70) Billamboz, N.; Grivet, M.; Foley, S.; Baldacchino, G.; Hubinois, J.-C. Radiolysis of the Polyethylene/Water System: Studies on the Role of Hydroxyl Radical. *Radiat. Phys. Chem.* **2010**, *79* (1), 36–40.
- (71) Gu, H.; Wu, J.; Doan, H. Hydrophilicity Enhancement of High-Density Polyethylene Film by Ozonation. *Chem. Eng. Technol.* **2009**, 32 (5), 726–731.
- (72) Ahn, Y.; Colin, X.; Roma, G. Atomic Scale Mechanisms Controlling the Oxidation of Polyethylene: A First Principles Study. *Polymers (Basel)* **2021**, *13* (13), 2143.
- (73) Oh, S.; Stache, E. E. Recent Advances in Oxidative Degradation of Plastics. *Chem. Soc. Rev.* **2024**, *53* (14), 7309–7327.
- (74) Zhang, K.; Han, L.; Nie, Y.; Szigeti, M. L.; Ishida, H. Examining the Effect of Hydroxyl Groups on the Thermal Properties of Polybenzoxazines: Using Molecular Design and Monte Carlo Simulation. *RSC Adv.* **2018**, *8* (32), 18038–18050.
- (75) Binda, G.; Zanetti, G.; Bellasi, A.; Spanu, D.; Boldrocchi, G.; Bettinetti, R.; Pozzi, A.; Nizzetto, L. Physicochemical and Biological Ageing Processes of (Micro)Plastics in the Environment: A Multi-Tiered Study on Polyethylene. *Environmental Science and Pollution Research* **2023**, *30* (3), 6298–6312.
- (76) Esmaeili Nasrabadi, A.; Babaei, N.; Bonyadi, Z. Effect of Ozonation on the Morphological Characteristics and Adsorption Behavior of Polystyrene Microplastics in Aqueous Environments. *Appl. Water Sci.* **2025**, *15* (5), 90.
- (77) Caputo, F.; Vogel, R.; Savage, J.; Vella, G.; Law, A.; Della Camera, G.; Hannon, G.; Peacock, B.; Mehn, D.; Ponti, J.; Geiss, O.; Aubert, D.; Prina-Mello, A.; Calzolai, L. Measuring Particle Size Distribution and Mass Concentration of Nanoplastics and Microplastics: Addressing Some Analytical Challenges in the Sub-Micron Size Range. *J. Colloid Interface Sci.* **2021**, *588*, 401–417.
- (78) Kumar, M.; Chaudhary, V.; Kumar, R.; Chaudhary, V.; Srivastav, A. L. Microplastics, Their Effects on Ecosystems, and General Strategies for Mitigation of Microplastics: A Review of Recent Developments, Challenges, and Future Prospects. *Environmental Pollution and Management* 2025, 2, 87–105.
- (79) Guidelines Approved by the Guidelines Review Committee. Guidelines for Drinking-Water Quality, 4th ed.; World Health Organization: Geneva, 2022.
- (80) Li, Y.; Li, J.; Ding, J.; Song, Z.; Yang, B.; Zhang, C.; Guan, B. Degradation of Nano-Sized Polystyrene Plastics by Ozonation or Chlorination in Drinking Water Disinfection Processes. *Chemical Engineering Journal* **2022**, 427, 131690.
- (81) Liu, P.; Lu, K.; Li, J.; Wu, X.; Qian, L.; Wang, M.; Gao, S. Effect of Aging on Adsorption Behavior of Polystyrene Microplastics for Pharmaceuticals: Adsorption Mechanism and Role of Aging Intermediates. *J. Hazard Mater.* **2020**, *384*, 121193.
- (82) Liu, B.; Jiang, Q.; Qiu, Z.; Liu, L.; Wei, R.; Zhang, X.; Xu, H. Process Analysis of Microplastic Degradation Using Activated PMS and Fenton Reagents. *Chemosphere* **2022**, 298, 134220.